Stem Cell Reports, Volume *14*

Supplemental Information

Pathogenic Pathways in Early-Onset Autosomal Recessive Parkinson's Disease Discovered Using Isogenic Human Dopaminergic Neurons

Tim Ahfeldt, Alban Ordureau, Christina Bell, Lily Sarrafha, Chicheng Sun, Silvia Piccinotti, Tobias Grass, Gustavo M. Parfitt, Joao A. Paulo, Fumiki Yanagawa, Takayuki Uozumi, Yasujiro Kiyota, J. Wade Harper, and Lee L. Rubin

Supplemental Figure 1

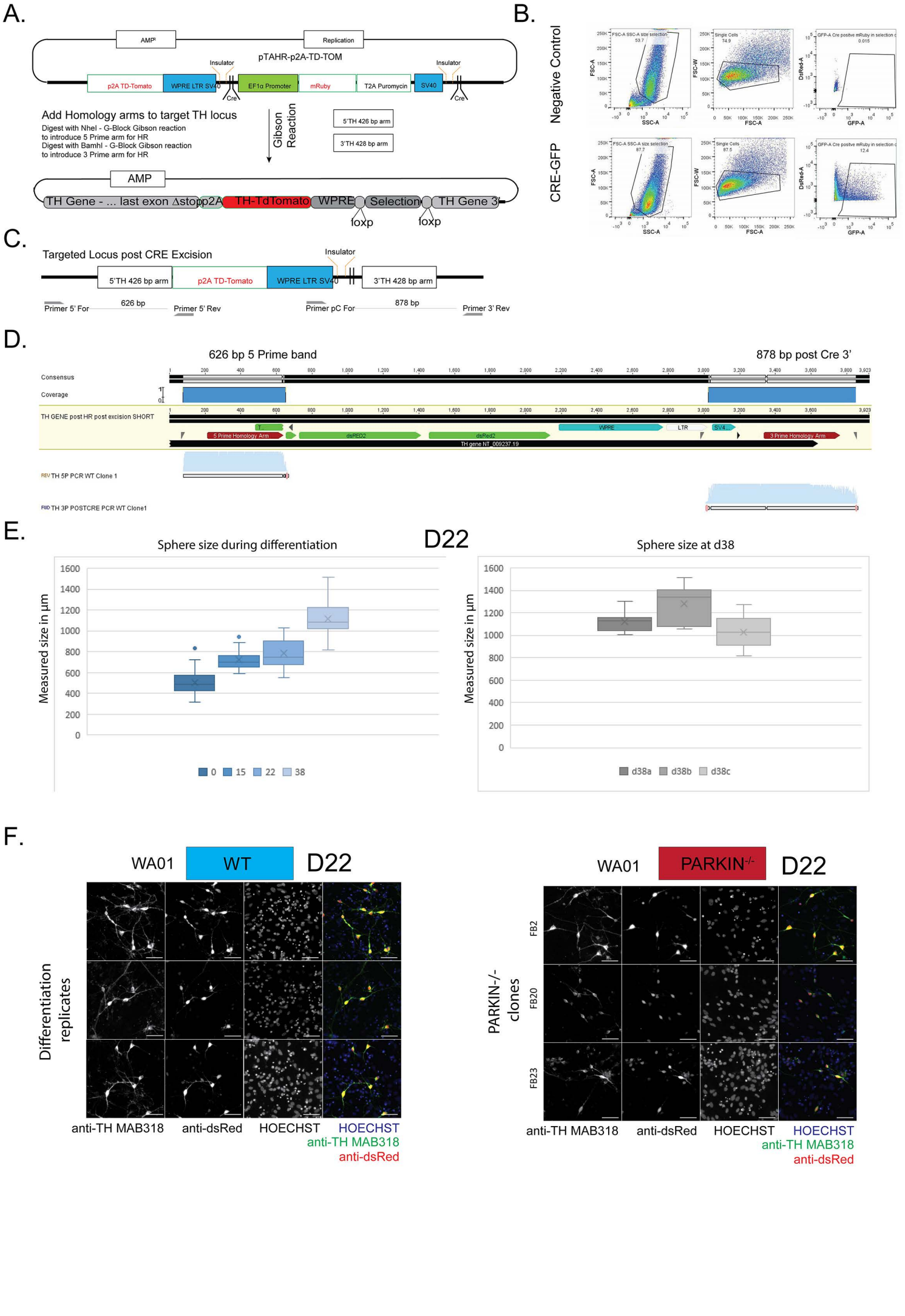

Supplemental Figure 2

A.

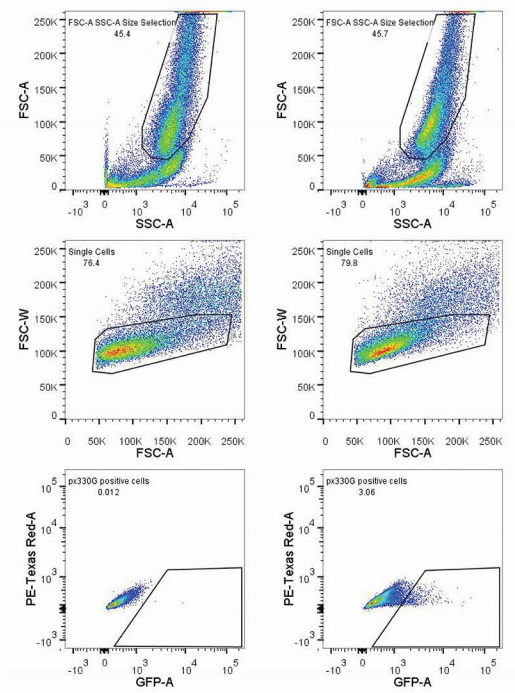

B.

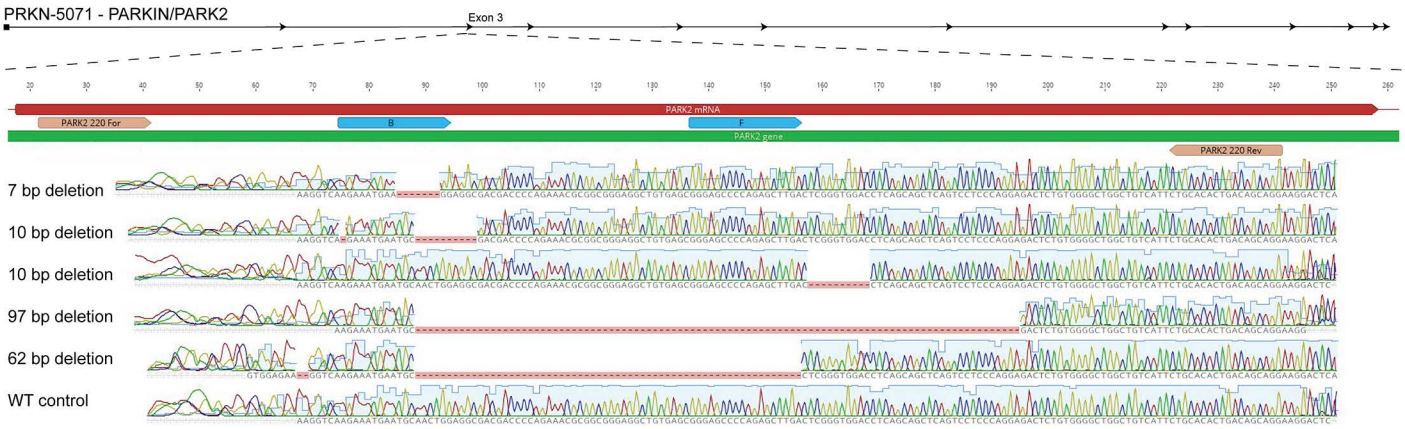

C.

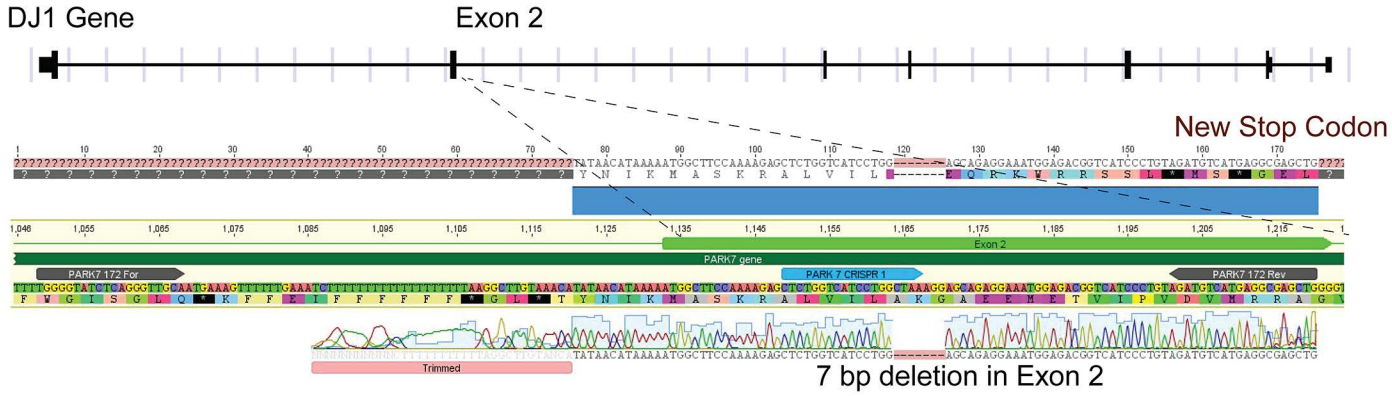

D.

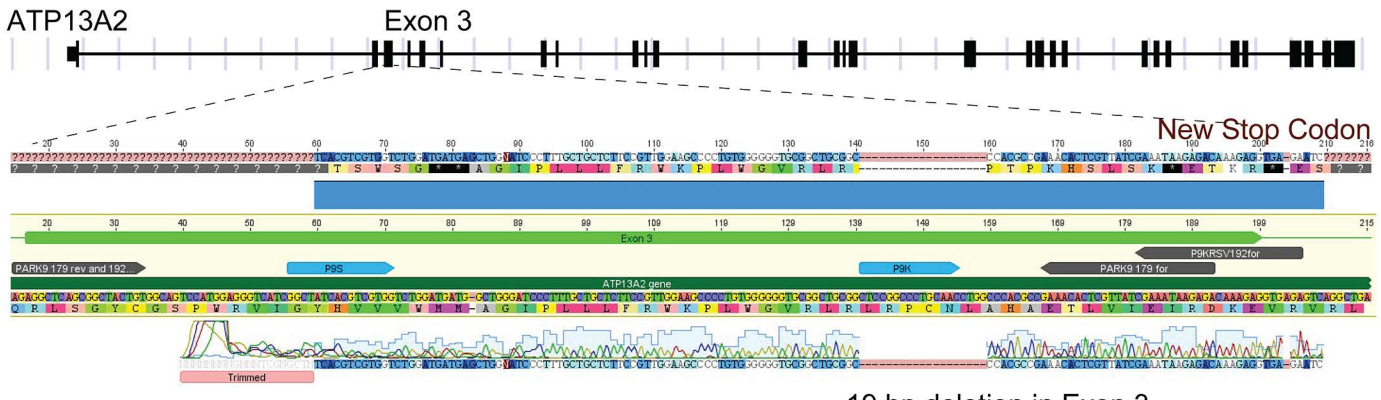

Supplemental Figure 3

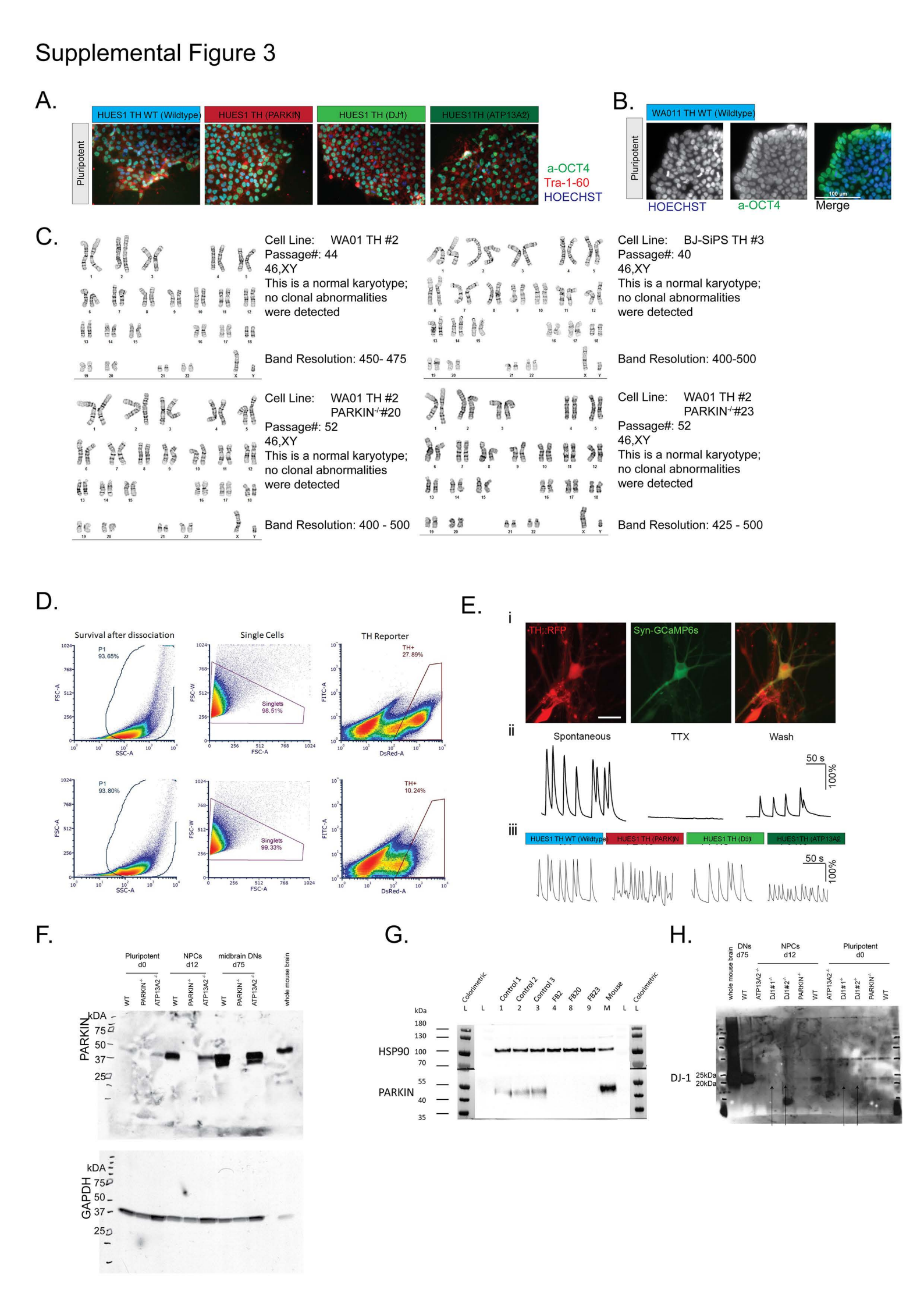

Supplemental Figure 4

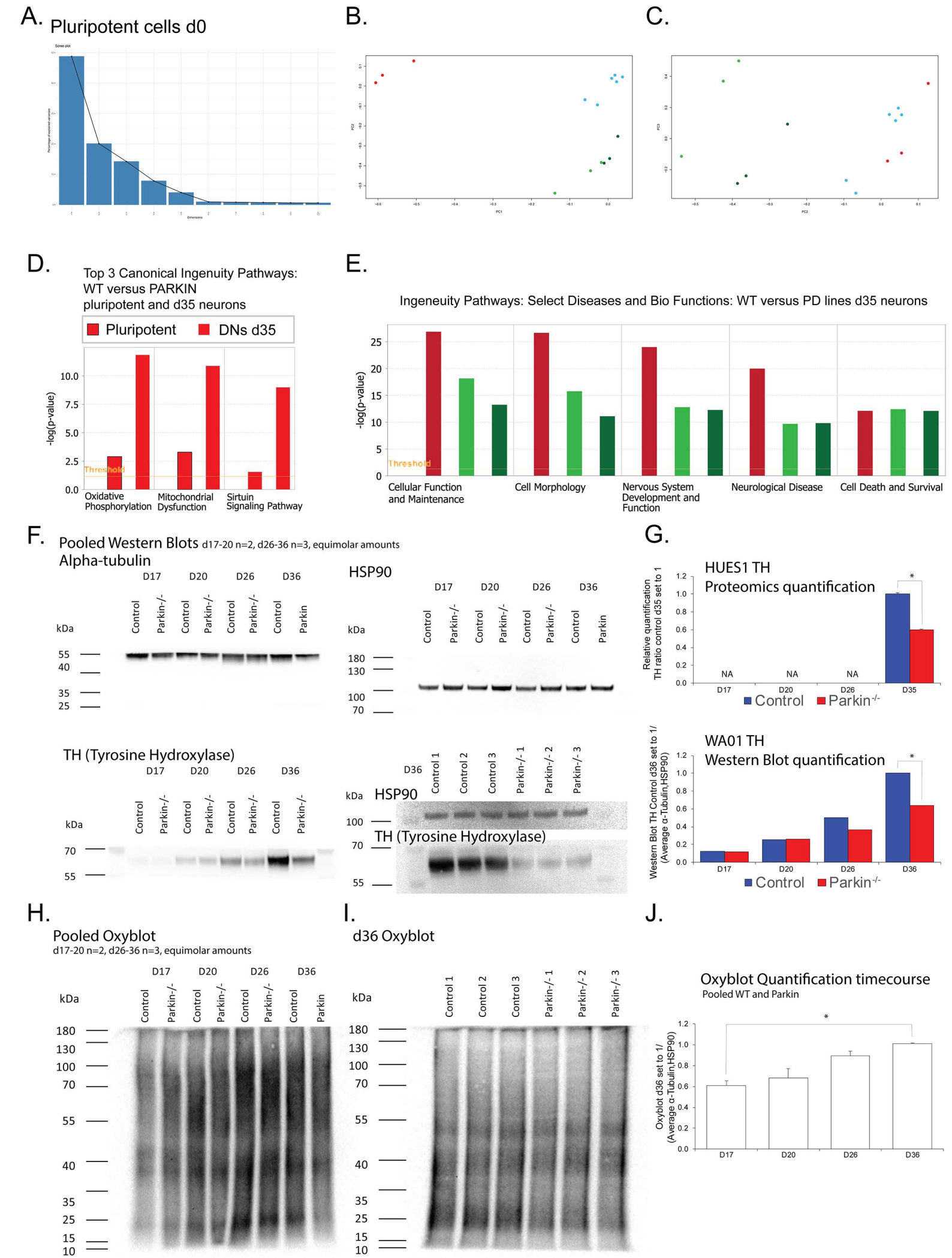

Supplemental Figure 5

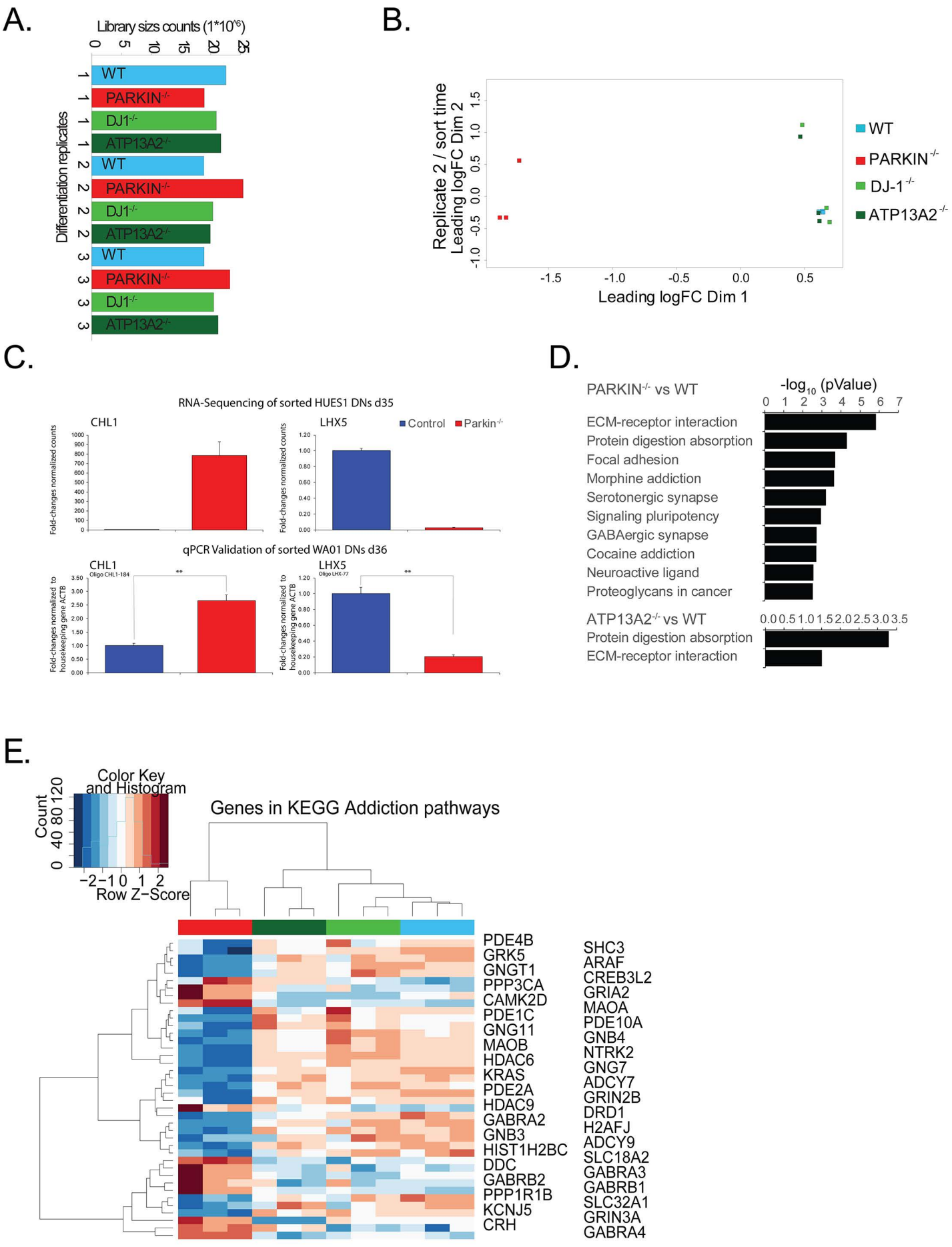

Pathogenic pathways in early onset autosomal recessive Parkinson's disease discovered using isogenic human dopaminergic neurons

Supplemental Figure 1 - Generation and Characterization of TH knock-in fluorescence reporter lines: A. Experimental scheme depicting the cloning steps taken to create basic targeting vector HR120-p2A-TdTomato as well as the additional Gibson reactions leading to the creation of the final targeting vector HR120-TH-p2A-TdTomato; B. Examples of FACS plots showing WT pluripotent control cells post nucleofection of $1*10^6$ cells with (top) vehicle control or (bottom) 5 µg CRE-GFP excision vector. A survival gate P1 was placed using FSC-A vs. SSC-A log parameters, a pulse geometry gate FSC-W vs. FSC-A was used to gate out doublets, and GFP^+ cells were sorted for clonal expansion; C. Scheme showing the PCR strategy to amplify the 5'-PCR as well as the 3'-PCR regions to confirm correctly targeted alleles; D. Potential TH-reporter knock-in clones were identified via PCR genotyping. PCR products were Sanger sequenced and aligned to the sequence expected after successful targeting; E. (left) WA01-TH WT cells were differentiated in spin culture and size was determined at d0, d15, d22, and d38, boxplots indicating size increase over time, centrality and range of spheres, (right) WA01-TH WT cells at d38 (n=3 independent differentiation experiments), boxplots indicating centrality and range of spheres; F. Fluorescence microscopy panel, showing d22 DNs dissociated on d15 and plated in low density on glial cells, from WA01-TH WT (left panel) and $PARKIN^{-/-}$ clones FB2, FB20 and FB23 (right panel). 20x Scale bar: 50 µm (left: a-TH (MAB318), middle left: a-dsRed, middle right: HOECHST, right: merge).

Supplemental Figure 2 - Derivation of isogenic cell lines: A. Examples of FACS plots showing WT pluripotent control cells post electroporation of $1*10^6$ cells with (left) vehicle control or (right) 5 µg CRISPR construct pX330 PARKIN. A survival gate P1 was placed using FSC-A vs. SSC-A parameters on log scale, a pulse geometry gate FSC-W vs. FSC-A was used to gate out doublets. mROS-G^+ cells were collected; B-D. Potential PD knockout clones were identified via PCR genotyping. PCR products were Sanger sequenced and aligned to the WT genotype; B. Potential *PARKIN* knockout clones showing exemplary mutations and proximity to guides used; C. Potential *DJ-1* knockout clones showing exemplary deletion in close proximity to the PARK7-CRISPR-1 binding site; D. Potential *ATP13A2* knockout clones showing exemplary deletion in close proximity to the PARK9-CRISPR-K binding site.

Supplemental Figure 3 - Validation of isogenic PD lines and characterization of derived DNs: A. Immunocytochemistry panel showing HUES1 isogenic reporter PD cell lines in the pluripotent state stained with TRA-1-60 (red), OCT-4 (green), and HOECHST (blue); B. Immunocytochemistry panel showing WA01-TH WT isogenic reporter cell line in the pluripotent state stained with OCT-4 (green) and HOECHST (blue); C. Karyotype analysis of WA01-TH WT, BJ-SIPS-TH WT, WA01-TH $PARKIN^{-/-}$-FB20 and $PARKIN^{-/-}$-FB23 lines; D. Dissociated spheres were analyzed via flow cytometry, examples of plots showing WA01-TH WT as well as $PARKIN^{-/-}$ lines at d22. A survival gate P1 was placed using FSC-A vs. SSC-A log parameters, a pulse geometry gate FSC-W vs. FSC-A was used to gate out doublets and TH:TdTomato number was quantified using gate P3; E. i) Live cell calcium imaging in TH^+ DNs derived from all 4 HUES1 lines by genetically encoded calcium indicator GCaMP6s. Sample fluorescence images showing GCaMP6s expression in TH^+ DNs. Scale bar: 50 µm; ii) Spontaneous calcium activities in WT DNs were blocked by incubation with sodium channel antagonist TTX (1 µM); iii) Sample intensity time plots showing spontaneous calcium activities in TH^+ DNs derived from all 4 HUES1 lines in culture medium; F. Image of full Western blot membrane corresponding to cropped images in Figure 2H. Western blot of HUES1 WT, $PARKIN^{-/-}$ and $ATP13A2^{-/-}$ lines using PARKIN antibody and GAPDH as a control at three timepoints (pluripotent state at d0, NPC at d12, and DN at d75). Mouse whole brain lysate was included as control; G. Western blot of WA01 WT and $PARKIN^{-/-}$ clones using PARKIN antibody and GAPDH as a control at d21. Mouse whole brain lysate was

used as control; H. Western blot of HUES1 WT, PARKIN$^{-/-}$, DJ-1$^{-/-}$, and ATP13A2$^{-/-}$ lines using DJ-1 antibody at three timepoints (pluripotent state at d0, NPC at d12, and DN at d75). Black arrows point to missing bands in the DJ-1$^{-/-}$ lines.

Supplemental Figure 4 - PCA of quantitative proteomics data in pluripotent cells and validation of dysregulated pathogenic pathways in HUES1-derived DNs (proteomics data): A-C. TMT proteomics results analyzed as relative abundances; A. Scree plot showing the percentage of variances explained by each principal component; B. PCA plot of components 1 and 2 at d35; C. PCA plot of components 2 and 3 at d35; D. Bar chart of d35 global proteomics comparisons between WT and all PARKIN$^{-/-}$ cell lines shows the top three dysregulated canonical ingenuity pathways using IPA curated sets. Y-axis shows the significance ($-\log_{10}$ (p-value)) and the orange line shows the significance threshold cut-off of $-\log_{10}$ (p-value = 0.05), sorted by significance in PARKIN$^{-/-}$ vs. WT comparison; E. Bar chart of d35 global proteomics comparisons between WT and all PD cell lines shows select altered disease or biological function pathways determined using IPA curated sets. Y-axis shows the significance ($-\log_{10}$ (p-value)) and the orange line shows the significance threshold cut-off of $-\log_{10}$ (p-value = 0.05), sorted by significance in PARKIN$^{-/-}$ vs. WT comparison; F. Top and bottom left: Western blot time-course analysis of WA01 WT and Parkin$^{-/-}$ samples for the housekeeping genes, alpha-tubulin and HSP90, as well as the DN marker, TH (pooled samples for display at d17 and d20 (n=2), d26 and d36 (n=3)). Bottom right: Western blot of WA01 WT and Parkin$^{-/-}$ triplicates at d36 for HSP90 and TH; G. Quantification of TH expression in pooled WA01 WT and Parkin$^{-/-}$ samples over time in comparison to d35 proteomics data from HUES1 lines, in the two genotype conditions. n=3, t-test * $p<0.05$; H. Western blot time-course analysis of pooled WA01 WT and Parkin$^{-/-}$ samples for protein carbonyl groups using the Oxyblot assay (pooled samples for display at d17 and d20 (n=2), d26 and d36 (n=3)); I. Western blot analysis of d36 WA01 WT and Parkin$^{-/-}$ triplicates for protein carbonyl groups using the Oxyblot assay; J. Quantification of protein carbonyls in pooled WA01 WT and Parkin$^{-/-}$ samples over time (n=2, t-test * $p<0.05$).

Supplemental Figure 5 - Transcriptomics Data: A. Sequencing library size in CPM (counts per million); B. Multi-dimensional scale plot of all isogenic cell lines in which distance corresponds to leading $\log_2$ fold changes between each pair of RNA samples. Dimension 1 separates the PARKIN$^{-/-}$ line from all other lines and dimension 2 separates replicate 2 from all other replicates; C. Validation of dysregulated pathogenic pathways in WA01 derived DNs (transcriptomics data). qRT-PCR analysis of sorted DNs at d36 shows dysregulation in CHL1 and LHX5 in HUES1- and WA01-derived DNs as mRNA fold change between the two genotype conditions (n=3, t-test ** $p<0.01$); D. KEGG pathway analysis showing top results for the enrichment analysis of differentially expressed transcripts in WT vs. PARKIN$^{-/-}$ and WT vs. ATP13A2$^{-/-}$ analyses (n=3); E. Heatmap across all samples using all genes associated with the KEGG term “addiction at the dopaminergic synapse.”

Supplemental Table 3 - FACS for TH percentage:

Name	Statistic	#Cells	Name	Statistic	#Cells
WT_1		50000	PARKIN_1		50000
FSC SSC	59.0	29511	FSC SSC	62.7	31347
Single Cells	95.3	28123	Single Cells	97.2	30483
TD Tomato high positive	41.3	11614	TD Tomato high positive	19.4	5914
WT_2		50000	PARKIN_2		50000
FSC SSC	63.2	31622	FSC SSC	66.6	33318
Single Cells	94.3	29823	Single Cells	96.7	32221
TD Tomato high positive	34.4	10261	TD Tomato high positive	16.8	5401
WT_3		50000	PARKIN_3		50000
FSC SSC	58.9	29474	FSC SSC	64.2	32100
Single Cells	96.3	28380	Single Cells	97.2	31190
TD Tomato high positive	30.1	8536	TD Tomato high positive	18.7	5825
WT_4		50000	PARKIN_4		50000
FSC SSC	55.5	27746	FSC SSC	62.0	30983
Single Cells	89.2	24751	Single Cells	97.1	30088
TD Tomato high positive	38.1	9429	TD Tomato high positive	16.7	5031
WT_5		50000	PARKIN_5		50000
FSC SSC	67.3	33653	FSC SSC	62.2	31102
Single Cells	91.3	30735	Single Cells	92.7	28835
TD Tomato high positive	28.2	8668	TD Tomato high positive	11.0	3184
WT_6		50000	PARKIN_6		50000
FSC SSC	66.7	33358	FSC SSC	66.3	33141
Single Cells	92.7	30937	Single Cells	94.8	31427
TD Tomato high positive	36.3	11243	TD Tomato high positive	17.4	5471
DJ-1_4		50000	ATP13A2_4		50000
FSC SSC	64.9	32458	FSC SSC	58.1	29026
Single Cells	96.3	31262	Single Cells	94.7	27495
TD Tomato high positive	29.1	9092	TD Tomato high positive	37.0	10173
DJ-1_5		50000	ATP13A2_5		50000
FSC SSC	68.4	34209	FSC SSC	66.3	33127
Single Cells	93.8	32085	Single Cells	93.7	31039
TD Tomato high positive	45.9	14726	TD Tomato high positive	47.4	14723
DJ-1_6		50000	ATP13A2_6		50000
FSC SSC	69.5	34737	FSC SSC	64.4	32218
Single Cells	93.3	32409	Single Cells	95.7	30848
TD Tomato high positive	44.7	14474	TD Tomato high positive	52.2	16092

Name	Count	Avg.	SD
WT	6	34.73333	4.922871791
P2F	6	16.66667	2.975679194
P7E	3	39.9	9.372299611
P9K	3	45.53333	7.770027885

	SS	DF
Between	2185.082778	3
Within	461.8733333	14
F	22.07759623	
P	**1.42445E-05**	****

Group 1	Group 2	Critical	P	Significant?
WT	P2F	0.008333	1.65563E-05	**Yes**
P2F	P9K	0.01	6.62576E-05	**Yes**
P2F	P7E	0.0125	0.000623274	**Yes**
WT	P9K	0.016667	0.035524519	No
WT	P7E	0.025	0.298858476	No
P7E	P9K	0.05	0.46777149	No

Supplemental Table 4 - CELLRox quantification:

Name	Count	Avg.	SD
WT TD TOMATO NEGATIVE GFP FSC SSC	4	1.355	0.50029991
WT TD TOMATO POSTIVE GFP FSC SSC	4	2.79	0.985731539
PARKIN TD TOMATO NEGATIVE GFP FSC SSC	4	6.0475	2.992349968
PARKIN TD TOMATO POSTIVE GFP FSC SSC	4	23.645	5.79446575
DJ-1 TD TOMATO NEGATIVE GFP FSC SSC	4	3.3875	2.071350204
DJ-1 TD TOMATO POSTIVE GFP FSC SSC	4	8.06	3.762516888
ATP13A2 TD TOMATO NEGATIVE GFP FSC SSC	4	4.3175	1.270206676
ATP13A2 TD TOMATO POSTIVE GFP FSC SSC	4	6.2375	1.512114965

	SS	DF
Between	1398.0047	7
Within	198.2967	24
F	24.17165274	
P	**2.09497E-09**	****

Group 1	Group 2	Critical	P	Significant?
WT TD TOMATO NEGATIVE GFP FSC SSC	PARKIN TD TOMATO POSTIVE GFP FSC SSC	0.001785714	0.000257769	**Yes**
WT TD TOMATO POSTIVE GFP FSC SSC	PARKIN TD TOMATO POSTIVE GFP FSC SSC	0.001851852	0.000393188	**Yes**
PARKIN TD TOMATO POSTIVE GFP FSC SSC	DJ-1 TD TOMATO NEGATIVE GFP FSC SSC	0.001923077	0.000589305	**Yes**
PARKIN TD TOMATO POSTIVE GFP FSC SSC	ATP13A2 TD TOMATO NEGATIVE GFP FSC SSC	0.002	0.000622833	**Yes**
WT TD TOMATO NEGATIVE GFP FSC SSC	ATP13A2 TD TOMATO POSTIVE GFP FSC SSC	0.002083333	0.00086095	**Yes**
PARKIN TD TOMATO POSTIVE GFP FSC SSC	ATP13A2 TD TOMATO POSTIVE GFP FSC SSC	0.002173913	0.001137469	**Yes**
PARKIN TD TOMATO NEGATIVE GFP FSC SSC	PARKIN TD TOMATO POSTIVE GFP FSC SSC	0.002272727	0.001668983	**Yes**
PARKIN TD TOMATO POSTIVE GFP FSC SSC	DJ-1 TD TOMATO POSTIVE GFP FSC SSC	0.002380952	0.004053602	No
WT TD TOMATO NEGATIVE GFP FSC SSC	ATP13A2 TD TOMATO NEGATIVE GFP FSC SSC	0.0025	0.004874896	No
WT TD TOMATO POSTIVE GFP FSC SSC	ATP13A2 TD TOMATO POSTIVE GFP FSC SSC	0.002631579	0.008762072	No
WT TD TOMATO NEGATIVE GFP FSC SSC	DJ-1 TD TOMATO POSTIVE GFP FSC SSC	0.002777778	0.012322761	No
WT TD TOMATO NEGATIVE GFP FSC SSC	PARKIN TD TOMATO NEGATIVE GFP FSC SSC	0.002941176	0.021295335	No
WT TD TOMATO POSTIVE GFP FSC SSC	DJ-1 TD TOMATO POSTIVE GFP FSC SSC	0.003125	0.035112571	No
WT TD TOMATO NEGATIVE GFP FSC SSC	WT TD TOMATO POSTIVE GFP FSC SSC	0.003333333	0.040865601	No
DJ-1 TD TOMATO NEGATIVE GFP FSC SSC	ATP13A2 TD TOMATO POSTIVE GFP FSC SSC	0.003571429	0.067954246	No
DJ-1 TD TOMATO NEGATIVE GFP FSC SSC	DJ-1 TD TOMATO POSTIVE GFP FSC SSC	0.003846154	0.072481277	No
WT TD TOMATO POSTIVE GFP FSC SSC	PARKIN TD TOMATO NEGATIVE GFP FSC SSC	0.004166667	0.084130695	No
ATP13A2 TD TOMATO NEGATIVE GFP FSC SSC	ATP13A2 TD TOMATO POSTIVE GFP FSC SSC	0.004545455	0.099819916	No
WT TD TOMATO NEGATIVE GFP FSC SSC	DJ-1 TD TOMATO NEGATIVE GFP FSC SSC	0.005	0.105052167	No
WT TD TOMATO POSTIVE GFP FSC SSC	ATP13A2 TD TOMATO NEGATIVE GFP FSC SSC	0.005555556	0.106157179	No
DJ-1 TD TOMATO POSTIVE GFP FSC SSC	ATP13A2 TD TOMATO NEGATIVE GFP FSC SSC	0.00625	0.108423685	No
PARKIN TD TOMATO NEGATIVE GFP FSC SSC	DJ-1 TD TOMATO NEGATIVE GFP FSC SSC	0.007142857	0.194106205	No
PARKIN TD TOMATO NEGATIVE GFP FSC SSC	ATP13A2 TD TOMATO NEGATIVE GFP FSC SSC	0.008333333	0.328113171	No
DJ-1 TD TOMATO POSTIVE GFP FSC SSC	ATP13A2 TD TOMATO POSTIVE GFP FSC SSC	0.01	0.403340847	No
PARKIN TD TOMATO NEGATIVE GFP FSC SSC	DJ-1 TD TOMATO POSTIVE GFP FSC SSC	0.0125	0.434522482	No
DJ-1 TD TOMATO NEGATIVE GFP FSC SSC	ATP13A2 TD TOMATO NEGATIVE GFP FSC SSC	0.016666667	0.473003452	No
WT TD TOMATO POSTIVE GFP FSC SSC	DJ-1 TD TOMATO NEGATIVE GFP FSC SSC	0.025	0.621068787	No
PARKIN TD TOMATO NEGATIVE GFP FSC SSC	ATP13A2 TD TOMATO POSTIVE GFP FSC SSC	0.05	0.913457289	No

Supplemental Table 1 - Proteomics Summary Table: Set 1: Intersection of d35 proteins, set 2: Intersection of pluripotent samples, all detected with confidence in two analyses that were bridged using WT-TH spheres from three independent differentiation replicates. Anova significance indicated with asterisk in column Anova, stringent pair-wise significance indicated in significance columns.

Supplemental Table 2 - Transcriptomics gene lists: Gene names as symbols, log fold changes (logFC), log counts per million (logCPM), likelihood ratio (LR), reported PValue, and false discovery rate (FDR) for all comparisons between WT and isogenic cell lines, cut-off FDR <0.01.

Supplemental Table 3 - FACS for TH percentage: Summarized table of propagated gates, FlowJo Table editor (FlowJo, LLC), FSC-A/SSC-A, and pulse geometry gate FSC-W/SSC-H. TH was quantified on a GFP-A/PE-Texas red-A gate.

Supplemental Table 4 - CellROX quantification: Summarized table of all CellROX quantification experiments, averaged mROS percentage, quantified as mROS-G^{+} using FlowJo synchronized bisector gates to divide the X-Axis into GFP^{-} and GFP^{+} non-overlapping populations based on the background expression in our unstained control (n=5, *p<0.05 ,**p<0.01). Statistical significance was analyzed by one-way ANOVA followed by Bonferroni-Holm multiple comparison test in independent staining and flow experiments, significance indicated in tables.

Supplemental Video 1 - Time-lapse video of HUES1 WT and PARKIN$^{-/-}$ cell lines between d15 and d21: Section 1. WT-Well-1 10x magnification; Section 2. WT-Well-1 representative area zoomed in; Section 3. PARKIN$^{-/-}$-Well-1 10x magnification; Section 4. PARKIN$^{-/-}$-Well-1 representative area zoomed in; Section 5. WT-Well-2 10x magnification; Section 6. WT-Well-2 representative area zoomed in; Section 7. PARKIN$^{-/-}$-Well-2 10x magnification; Section 8. PARKIN$^{-/-}$-Well-2 representative area zoomed in.

Experimental Procedures:

Dissociation of differentiated spheres

Before dissociation, HUES1 spheres were collected from spinner flasks and incubated for 1 hour in BAGTC+ 5 µM ROCK inhibitor. Spheres were transferred into falcon tubes and settled by gravity. After washing with PBS, cells were incubated for ~10 min. in 1 ml Accutase under constant manual shaking at 37°C. When spheres appeared less tight, the enzymatic digest was stopped by adding 5 ml of BAGTC+ 0.25 mg/ml DNase (Worthington Biochemical) and cells were gently triturated using a 5-ml pipette. Cells were spun at 800 RPM for 5 min. and resuspended in 1 ml BAGTC+ 5 µM ROCK inhibitor and triturated 10 times before getting filtered through a 70-µm mesh. For the WA01 cell lines, spheres were collected from spinner flasks into 12-well plates and incubated for 1 hour in BAGTC+ 10 µM ROCK inhibitor. After washing with PBS, cells were incubated for ~20 min. in 2 ml/well Accutase under constant manual shaking at RT. When spheres appeared less tight, they were gently triturated using a 5-ml pipette, followed by a 1 ml pipette tip. The dissociated spheres were transferred to 15 ml tubes containing 10 ml FACS buffer (BAGTC+ 10 uM ROCK inhibitor + 0.25 mg/ml DNase + 2% bovine calf serum (HyClone)) to stop the enzymatic digest, filtered through a 70-µm mesh and spun at 500 g for 5 min. at RT. The pellets were resuspended in 0.5 ml FACS buffer (for FACS experiments) or BAGTC+ 10 µM ROCK inhibitor (for plating) and filtered through a 0.35-µm mesh. Cells were counted using Bio-Rad cell counter and live cell dye Trypan blue. For long term culture of dissociated spheres, cells were plated on Poly-L-Lysine protein coated 96-well microplates (Greiner) coated with 1 µg/mL laminin and mouse glia (C57BL/6 Sciencell Research Laboratories #M1800-57 or CD1) at a seeding

density of 50,000 cells. For short-term imaging experiments the same plates and coatings were used, and dissociated cells were seeded at appropriate densities.

Generation of isogenic knockout lines

Human ESCs were cultured in standard conditions, and, prior to electroporation, cells were pre-treated for 1 hour with 10 μM ROCK inhibitor. $4*10^6$ cells were dissociated using Accutase (diluted at 1:3 in calcium- and magnesium-free PBS ($PBS^{-/-}$)). Cells were pelleted and resuspended in 800 μl $PBS^{-/-}$ containing 5 μg px330 CRISPR DNA or using two CRISPRs (2.5 μg each) and transferred into electroporation cuvettes. Electroporation was carried out using the Gene Pulser Xcell™ Electroporation Systems and standard settings, 250 V and 500 μF. Alternatively, nucleofection was carried out using either the P3 Nucleofector kit from Amaxa and the standard program CB-150 or the primary P4 Nucleofector kit from Amaxa and the standard program hiPSC CA137. Cells were sorted for GFP 24 hours post perturbation. GFP^+ cells were plated at clonal densities (20 cells/cm^2). Colonies were picked and expanded as clonal lines. At least 96 clones were analyzed per cell line. Genotyping PCR was used to identify clones with homozygous or compound heterozygous deletions leading to truncations and frameshift mutations. Clones for all three lines containing deletions were identified by Sanger sequencing.

Generation of the TH:TdTomato targeting vector

The final vectors were derived through modifications of the commercially available HR120-PA-1 vector (https://www.systembio.com/genome-engineering-precisionx-HR-vectors/gene-tagging). To create a new multicistronic vector, the copGFP-polyA cassette was removed using EcoRI and NruI. Vector sequence was restored via G-Block cloning which introduced a P2A cassette. The 2A self-cleaving peptide sequence is used to separate the TH protein from the TdTomato and to retain a largely unaltered endogenous TH gene product (Figure S1A). In subsequent steps the XhoI site and Gibson assembly were used to introduce the fluorophore coding sequence (CDS) followed by the Woodchuck Hepatitis virus post-translational response element (WPRE) to enhance mRNA stability and translation. For example, the TdTomato CDS followed by the WPRE element was amplified using pFUGW-TdTomato as a template. The PCR product was inserted via Gibson cloning. To add 5' homology arms to the HR120-p2A-TD-TOM, the vector has to be cut with the restriction endonuclease NheI. A homology arm is created either by PCR or DNA synthesis utilizing 18-40 bp long overlap sequences between the vector and insert. A template for the DNA generation is given below. Vector and homology arm are enzymatically assembled using Gibson reaction. In a subsequent step, BamHI restriction endonuclease can linearize the vector to add a 3' homology arm. The 5' homology arm ends before the stop codon of the gene of interest to allow for a fusion protein or multicistronic expression. The necessary overhangs are shown in detail in Table 1. In the case of the TH targeting vector (TH-HR120-TdTomato-WPRE), we used ~500-bp sequences with homology to the targeted *TH* locus that can act as homology arms. After the removal of the stop codon, the last exon of the *TH* gene is fused to an in-frame p2A-TdTomato sequence followed by the WPRE site and a loxP-flanked drug-resistance cassette (Figure S1A).

Table 1 - Nucleotide sequence that can be used to create overlapping sequence for Gibson assembly

HR120-p2A-TdTomato:	NheI and BamHI
GACGTTGTAAAACGACGGCCAGTGAATTCAGCTAG	5 Prime 1st overhang (NheI digest)

GCTAGCGGAAGCGGAGCTACTAACTTCAGCCTGTTGA	5 Prime 2nd overhang (NheI digest)
CACGTAAGTAGAACATGAAATAACCTAGATCGGATC	3 Prime 1st overhang (BamHI digest)
GATCCCCGTCGACTGCATGCAAGCTTGGCGTAATC	3 Prime 2nd overhang (BamHI digest)

Generation of TH-reporter knock-in lines

Nucleofection was carried out using either the P3 Nucleofector kit from Amaxa and the standard program CB-150 or the primary P4 Nucleofector kit from Amaxa and the standard program hiPSC CA137. Best nucleofection conditions were different using two Amaxa 4D-Nucleofector™ X units. 1-2*10^6 cells were dissociated using Accutase (diluted at 1:3 in $PBS^{-/-}$). Cells were pelleted and resuspended in 100 µl nucleofection solution loaded with two different CRISPR constructs (2 µg px330 CRISPR DNA each) plus 5 µg targeting vector and transferred into electroporation cuvettes. To improve the odds of successful targeting, we created CRISPR/Cas9 constructs by cloning CRISPR guide sequences into the pX330 Cas9 plasmid (Cong et al., 2013). We selected CRISPR guide sequences that were located on opposite strands overlapping with the stop codon of the *TH* gene. Guides were designed to exhibit overlapping sequences in both homology arms to prevent binding of the CRISPR to the targeting vector. Cells were recovered in mTESR on plates pre-coated with Matrigel. After nucleofection of hPSCs with both TH-CRISPR-Cas9 expression vectors as well as the pHR120-TH:TdTomato-WPRE plasmid (Figure S1A), they were cultured in the presence of Puromycin for 2 days. We then observed the emergence of Puromycin-resistant clones that maintained hPSC-like morphology. Cells were allowed to grow to confluency. To excise the selection cassette, we nucleofected mixed clones containing 100 to 200 selected colonies with pCAG-Cre:GFP (Matsuda and Cepko, 2007). To enrich for cells that received the CRE plasmid, we enriched for GFP^+ cells using flow sorting (Figure S1B). We expanded 24 clonal cell lines. Post Cre excision we screened for homologous recombination and correct gene insertion using primers outside the targeting arm and inside the targeting vector (Figure S1C). The 5'-PCR yielded a strong PCR band of 626 bp size while the 3'-PCR showed the expected band size at 878 bp. We used Sanger sequencing to analyze the resulting PCR products (Figure S1D).

Electrophysiology and calcium imaging

As previously described (Eden et al., 2009; Rigamonti et al., 2016), whole-cell patch clamp recordings were performed with a Multiclamp 700B amplifier and a Digidata 1550 Digitizer (Molecular Devices). Data were collected using pClamp 10 software (Molecular Devices), sampled at 10 kHz, and filtered at 1 kHz. Cells were continually perfused with Tyrode's solution at RT: 128 mM NaCl, 30 mM glucose, 25 mM HEPES, 5 mM KCl, 2 mM $CaCl_2$, and 1 mM $MgCl_2$ (adjusted to pH 7.3 with NaOH). Patch pipettes were pulled from borosilicate glass using a P-1000 Micropipette Puller (Sutter Instrument) with resistance of 4-8 MΩ when filled with pipette solution containing: 147 mM KCl, 5 mM Na_2-phosphocreatine, 2 mM EGTA, 10 mM HEPES, 2 mM MgATP, and 0.3 mM Na_2GTP (adjusted to pH 7.3 with KOH). For voltage-clamp recordings, membrane potential was held at -70 mV. For current-clamp recordings, resting membrane potential was adjusted to -60 mV by a small current injection. For sodium/potassium current recordings, membrane potential was depolarized from -60 mV to 50 mV in 10 mV increments.

Live cell calcium imaging

DNs were seeded on top of CD1 mouse cortical astrocytes after flow sorting and infected with AAV1-Syn-GCaMP6s (Penn Vector Core, #AV-1-PV2824). Live cell imaging with perfusion was performed on a Nikon Eclipse Ti-S Inverted microscope with a perfusion chamber. Cells were continuously perfused with Tyrode's solution at RT. Time-lapse recordings were acquired at 1 frame per second with a 20x objective. Mean fluorescent intensity of GCaMP6s was measured in cell soma by ImageJ (U.S. National Institutes of Health, http://imagej.nih.gov/ij/), normalized to the minimal intensity, and plotted by Igor (WaveMetrics).

Flow analysis and FACS of midbrain DNs

To assess the percentage and create pure cultures of TH^+ cells, spheres were analyzed using a BD LSR-II analyzer and sorted using a BD FACSAria II flow sorter. Cells were dissociated and counted and medium adjusted to contain no more than 2 million cells per ml and transferred into Falcon® 5-mL round-bottom Polystyrene test tubes, with cell strainer snap caps and run on the 15-parameter BD FACSAria II+, customized for small particle to average cell (<0.1 microns) sorting using a low-pressure nozzle and custom settings. Forward scatter (FSC) and side scatter (SSC) were used to eliminate debris in conjunction with FSC-width (FSC-W) and SSC-area (SSC-A) to focus on single cells. TdTomato fluorescence vs. GFP fluorescence was used to select TH^+ cells and remove dead cells (auto-fluorescence in the green channel). Data was analyzed using FlowJo or FCS express software. Dissociation of tight neurospheres is a critical step as the process will inevitably lead to cell death and debris. Debris and dead cells typically have a lower level of FSC-A and SSC-A which are found in the lower left part of the scatter plot (Figure S2A, left panel). We gated to exclude most dead cells and debris. We used a pulse geometry gate FSC-W and SSC-height (SSC-H) to gate out doublets (Figure S2A, middle panel). We quantified TH expression on a GFP-A PE-Texas red-A gate against a negative pluripotent control (Figure S2A, right panel and Table S3). Usually, we performed experiments in triplicates. Some experiments were quantified using more differentiation replicates. We repeated the quantification of TH^+ neurons at d35 in 6 (WT and $PARKIN^{-/-}$ lines) and 3 ($DJ\text{-}1^{-/-}$ and $ATP13A2^{-/-}$ lines) independent differentiations. To measure CellROX positivity, we performed a total of 4 differentiation experiments for each line and stained independently twice. CellROX exhibits green fluorescence upon oxidation by mROS with an absorption/emission maximum of ~485/520 nm. In a histogram, we overlaid results from the unstained control, the WT line and the $PARKIN^{-/-}$ line (Figure 3E). In our flow cytometry analysis of the cells, we gated on TH^+ and TH^- cells and measured GFP intensity (Table S4).

Nikon BioStation CT imaging

For live cell imaging in the Nikon BioStation CT, we dissociated all isogenic lines at d15. We determined live cell numbers using an automated cell counter and Trypan blue staining and plated $5x10^4$ unsorted live cells per well for each cell line into a 96-well plate pre-coated with mouse glia at a seeding density of 50,000 cells. In previous experiments, we found almost uniform expression of the NPC marker NESTIN in our cultures at this time, with approximately 5% of the cells expressing TdTomato. We began image acquisition at d16, 24 hours post dissociation. Images were acquired every 6 hours over 8 days until d25 of differentiation.

Immunocytochemistry

Cells were fixed with either 5% PFA or cold methanol (-80°C) as indicated in Table 2. Cells were blocked in 0.1% Triton X-100 (Sigma) in 5% horse serum/PBS, and then incubated in primary antibody (0.1% Triton X-100 in 5% horse serum/PBS) overnight at 4°C. On the following day, cells

were washed in PBS-T, incubated in species-specific fluorophore conjugated Alexa fluor secondary antibodies and HOECHST nuclear stain according to the manufacturer's protocol.

Table 2 – Antibodies used for immunocytochemistry experiments.

Company	Target	Antibody
Abcam	TRA-1-60	ab16288
Abcam	OCT4	ab19857
Abcam	FOXA2	ab60721
Abcam	LMX1A	ab139726
Pel Freez	TH	P40101-0
Millipore	TH	MAB318
VWR	RFP	RL600-401-379

IHC and image analysis of sectioned spheres:

Serial sections (4-6 µm) of paraffin-preserved midbrain organoid sections were prepared using a Leica RM2255 microtome and used for IHC analysis. Organoids from the WA01-TH WT cell line were fixed with 4% PFA for 5 min. and embedded on d0, d15, d22, and d38 of differentiation. Sections were placed on charged slides and baked overnight at 70°C. IHC was performed on Ventana Benchmark XT. Antigen retrieval with CC1 (citric acid buffer) was performed for 1 hour followed by primary antibody incubation for 30 min. The primary antibodies used are listed in Table 3. A multimer secondary antibody was used for all samples. IHC sections were imaged using a Nikon Eclipse Ci-L equipped with a Nikon Digital Sight DS-Fi2 camera. Live d22 spheres from the BJ-SIPS-TH WT cell line were imaged using spinning disc confocal CX7. Maximum projections were generated using z-stack images that were acquired in laser confocal mode in 10x magnification, pin hole size 70.

Table 3 – Antibodies used for IHC experiments.

Company	Target	Antibody
Thermo Fisher Scientific	TRA-1-60	41-1000
Cell Signaling Technology	OCT4	2750
Abcam	FOXA2	ab60721

Sigma	LMX1A	HPA030088
Pelfreeze	TH	P40101-150
Millipore	TH	MAB318
Rockland	RFP	600-401-379

Karyotype analysis

We utilized Giemsa stained mitotic chromosome preparation (G-banding) to screen for genomic abnormalities (>5-10 Mb), inversion, duplications, deletions, translocations or aneuploidies in WT-TH cell lines and select clones. The analysis was performed by the WiCell cytogenetics laboratory with protocols optimized for hPSCs. Twenty metaphase spreads were analyzed for each sample. Karyotypic abnormalities are frequently discovered after genome editing and selection in hPSCs. We made large freezes of cells prior to karyotyping and routinely return to low passage stocks to avoid working with cells that may acquire chromosomal changes post analysis. WA01-TH and BJ-SIPS-TH cell lines and selected clones were normal as indicated. Karyotype analysis in the original HUES1-TH WT donor cell line revealed an extra copy of the short-arm of chromosome 12 from band p13.33 to p11.1 and loss of the short-arm of chromosome 10 from band p14 to p12.2 typical for survival and growth advantage of pluripotent stem cells. The abnormalities were propagated in isogenic descendants.

RNA extraction

WA01 derived DNs were sorted on d36 for RNA extraction using the Monarch Total RNA Miniprep Kit (NEB). The SuperScript IV First-Strand Synthesis System (Invitrogen) was then used to prepare the cDNA samples.

qRT-PCR

The qRT-PCR mixes were loaded with SYBR Green PCR Master Mix (Applied Biosystems) for analysis using the QuantStudio System (Applied Biosystems). qRT-PCR primers were designed to be exon spanning (Table 4). We chose highly dysregulated genes that were identified in the transcriptomics studies of HUES1 WT and Parkin$^{-/-}$ cell lines. Here, we differentiated WA01 WT and Parkin$^{-/-}$ cells in three independent experiments. We then sorted the DNs at d36 and performed qRT-PCR. We tested CHL1 and LHX5 expression that showed strong dysregulation between WT and Parkin$^{-/-}$ lines and could successfully be amplified via qRT-PCR (Figure S5C). Both recapitulated the expected dysregulation in the same direction. CHL1 likely plays a role in cell adhesion and synaptic function and has not been investigated in the context of Parkin dysregulation but has been discussed as a risk gene for Parkinsonism (Pottier et al., 2018). We interpreted the presence of LHX5 as incomplete midbrain patterning. Cells that receive too little WNT signaling show hypothalamic LHX5 expression in our system. It is unclear whether the reduced transcript abundance in the Parkin$^{-/-}$ line represents a type of survival or differentiation bias, but the data are consistent across cell lines.

Table 4 - The primer sequences used for qRT-PCR analysis.

LHX5	Forward primer	GTTCGTGTGCAAAGACGACTAC
	Reverse primer	CCGTACAGGATGACACTGAGTT
CHL1	Forward primer	TGGCATCTTGTTATGTGAGGCT
	Reverse primer	TCCATGGACATTTGAGGCTTCA
ACTB	Forward primer	ACCGGGCATAGTGGTTGGA
	Reverse primer	ATGGTACACGGTTCTCAACATC

Western blotting

Cell culture lysates were generated using RIPA Lysis and Extraction Buffer (Thermo Fisher Scientific), or 2% SDS lysis buffer (50 mM tris, 100% glycerol, and 10% SDS) containing protease inhibitor cocktail (100x; Roche) and phosphatase inhibitor cocktail (100x; Abcam), or 18% SDS lysis buffer (1 M tris-HCl (pH 6.8), 8 M urea, 20% glycerol, and 18% SDS). Protein concentration was estimated using the Pierce BCA Protein Assay Kit (Thermo Fisher Scientific). For Western blot analysis 20-40 µg total protein was denatured under reducing conditions in 4x Laemmli Sample Buffer (Bio-Rad) by boiling in 4X Bolt LDS Sample Buffer (Novex) for 10 min. at 98°C prior to loading onto a 10% Criterion TGX Precast gel (Bio-Rad) or a NuPAGE 4-12% Bis-Tris Gel (Invitrogen), then transferred to a PVDF or nitrocellulose membrane (0.22 µm; Bio-Rad or Novex) using the Criterion Blotter system (Bio-Rad) or iBlot 2 dry blotting system (Invitrogen). Membranes were blocked for 1 hour at RT in 5% w/v non-fat milk (Santa Cruz) or BSA (Sigma) in TBS containing 0.1% v/v Tween-20 (Fisher Scientific; TBS-T). Membranes were then incubated in the indicated primary antibody (in 5% milk or BSA/TBS-T) overnight at 4°C, washed 4 times in TBS-T, incubated in species-specific HRP-conjugated secondary antibody (in 5% milk or BSA/TBS-T) for 1 hour at RT, and then washed 4 times in TBS-T. Membranes were subsequently developed with ECL Western blotting substrate (Pierce or PerkinElmer) and immunodetection was performed using the ChemiDox XRS$^+$ System (Bio-Rad). Membranes were then washed once in TBS-T and stripped in stripping buffer (25 mM Glycine HCl, pH 2.0 and 1% w/v SDS) with vigorous shaking to remove primary and secondary antibodies, washed three times in TBS-T, and blocked for 1 hour (in 5% milk/TBS-T) at RT before probing with the next primary antibody. The antibodies used are listed in Table 5.

Table 5 – Antibodies used for Western blots experiments.

Company	Target	Antibody
Santa Cruz	PARKIN PRK8	sc-32282
Abclonal	DJ-1 PARK7	A0987
Thermo Fisher Scientific	GAPDH	4300
Cell Signaling Technology	HSP90	4874

Semi-quantitative Western blot to determine TH expression

Samples of midbrain DN spheres were collected at specific timepoints for protein extraction, quantification, and Western blot analysis as described above. The results were quantified using Image Studio Lite (LI-COR Biosciences). To validate that TdTomato expression is reflective of TH expression and to confirm the quantified reduced TH expression in quantitative proteomics experiments, we employed Western blot techniques using the developmental timepoints d17, d20, d26, and d36 in three independent differentiation experiments of WA01 WT and Parkin$^{-/-}$ lines. We pooled differentiation experiments for display of developmental timepoints using equimolar inputs. We first tested several housekeeping genes in a time-course. Alpha-tubulin and HSP90 show consistent expression across samples and timepoints (Figure S4F, top panel). We used an average of these housekeeping genes for all normalizations and quantifications. In line with our flow cytometry findings, TH expression increased over time during terminal differentiation (Figure S4F, bottom left panel). HPS90 and TH expression is also shown for individual samples at d36 (Figure S4F, bottom right). Experiments in the HUES1 cell line showed that TH protein abundance is about 50% lower in Parkin$^{-/-}$ cells using iTRAQ relative quantification of protein abundance (Figure S4G, top panel). Here we confirm the significantly reduced TH protein expression at d35 in independent WA01 derived Parkin$^{-/-}$ cells (Figure S4G, bottom panel).

Table 6 - The primary and secondary antibodies used for semi-quantitative Western blot analysis.

Primary antibody	Company	Catalog Number	Dilution
Alpha-tubulin	Sigma-Aldrich	T6074	1:4000
HSP90	Cell Signaling	4874S	1:10,000
Tyrosine hydroxylase	Millipore	MAB318	1:1000
Secondary antibody			
Anti-mouse	Jackson IR	715-035-150	1:10,000
Anti-rabbit	Jackson IR	711-035-152	1:10,000

Oxyblot assay

Protein carbonyl groups of individual or pooled whole lysates were derivatized with DNP using the OxyBlot Protein Oxidation Detection Kit (EMD-Millipore) reagents and conditions according to the manufacturer. To validate that OS is connected to DN physiology, we utilized the Oxyblot techniques in a time-course experiment as well as on d36 (Figures S4H-I). Oxyblots measure protein carbonyl content, which is considered a marker of oxidative modification of proteins and, therefore, of OS (Butterfield et al., 2010). In a series of experiments using this method, we found that the quantity of carbonylated proteins in differentiating hPSCs increased over time and was significantly different between d17 and d35 (Figure S4J). We believe that this observation reflects the unique properties of DNs and their well-known oxidation of dopamine in response to OS (Burbulla et al., 2017; Surmeier et al., 2017). However, we did not observe a significant increase of protein carbonylation in Parkin$^{-/-}$ midbrain spheres compared to WT controls. At the time of the experiments, WA01 Parkin$^{-/-}$ spheres contain fewer than half the number of TH^{+} DNs. Thus, we hypothesize that the Parkin$^{-/-}$ DNs likely experienced more OS per neuron, but that was balanced by a reduced number of DNs in the spheres. Future experiments using sorted DNs or inhibition of TH during the differentiation might increase our understanding of this mechanism.

mRNA-Seq library preparation and sequencing

RNA extraction for mRNA sequencing was performed post flow sorting of at least 200,000 TH^+ cells using Qiagen micro RNA extraction with on-column DNase digest. RNA amount and integrity were approximated using the bioanalyzer 2100 RNA Nano kit. Illumina mRNA-seq libraries were prepared using the TruSeq RNA kit using 200 ng of total RNA per sample. Library sequencing was carried out on a HiSeq2500 in rapid mode, 1 lane/pool. Each pool contained 6 samples, 3 differentiation replicates per isogenic cell line. The concentration of both pools was approximately 2.6 ng/µl and each library was sequenced to a depth of ~60 million fragments using 50 bp paired-end reads. RNA-seq reads were mapped using TopHat version 2.0.9 against the human genome build GRCh38. The primary assembly was downloaded from primary assembly from ftp://ftp.ensembl.org/pub/release-85/fasta/homo_sapiens/dna/.

Gene expression analysis

FASTQ files were aligned to the primary assembly ENSEMBL GRCh38 index built ftp://ftp.ensembl.org/pub/release-85/fasta/homo_sapiens/dna/ using Tophat. For annotations, we used a GTF transcriptome build GRCh38 here: ftp://ftp.ensembl.org/pub/release-85/gtf/homo_sapiens. Gene expression analysis was carried out with the statistical software R and several Bioconductor packages including edgeR (McCarthy et al., 2012; Robinson et al., 2010). Data was normalized using standard edgeR parameters. We excluded low count genes (less than 30 counts in at least 2 conditions). Using the generalized linear modeling framework of edgeR, we identified DEGs between all experimental conditions. Multiplicity correction applying the Benjamini-Hochberg method was performed on the p-values, to control the FDR (false discovery rate). Table S2 contains original countable and pairwise comparisons between WT and isogenic PD lines. Log-fold changes and FDRs.

Proteomics - Cell lysis and protein digestion

Cells were lysed in 8 M urea and 50 mM EPPS with sonication. The homogenate was sedimented by centrifugation at 21,000 x g for 5 min. Proteins were subjected to disulfide bond reduction with 5 mM tris(2-carboxyethyl)phosphine (RT, 30 min.) and alkylation with 10 mM chloroacetamide (RT, 30 min. in the dark). Methanol-chloroform precipitation was performed prior to protease digestion. Samples were resuspended in 200 mM EPPS (pH 8.5) and digested at RT for 13 hours with LysC protease at a 100:1 protein-to-protease ratio. Trypsin was then added at a 100:1 protein-to-protease ratio and the reaction was incubated for 6 hours at 37°C.

AQUA proteomics

For AQUA/PRM, samples were subjected to Trichloroacetic acid (TCA) precipitation. Samples were first digested with Lys-C (in 100 mM tetraethylammonium bromide (TEAB), 0.1% Rapigest (Waters Corporation), 10% (vol/vol) acetonitrile (ACN)) for 2 hours at 37°C, followed by the addition of trypsin and further digested for 6 hours at 37°C. Digests were acidified with an equal volume of 5% (vol/vol) formic acid (FA) to a pH of ~2 for 30 min., dried down, and resuspended in 1% (vol/vol) FA.

For PARKIN AQUA/PRM, three heavy-labeled reference peptides (QGVPADQL**R**; ILGEEQYN**R**; VCMGDHW**F**DV – where Cysteine is carboxyamidometylated and Methionine oxidized), each containing a single 13C/15N-labeled amino acid (indicated in bold and underlined), was produced at Cell Signaling Technologies and quantified by amino acid analysis. AQUA peptides from working stocks (in 5% (vol/vol) FA) were diluted into the digested sample (in 1% (vol/vol) FA) to be analyzed to an optimal final concentration predetermined for individual peptides. Samples and AQUA peptides were oxidized with 0.05% hydrogen peroxide for 20 min. at RT, subjected to C18 StageTip, and resuspended in 1% (vol/vol) FA. MS data were collected sequentially by LC/MS on an Orbitrap Fusion Lumos mass spectrometer (Thermo Fisher Scientific) coupled to a Proxeon EASY-nLC 1200 liquid chromatography (LC) pump (Thermo Fisher Scientific). The capillary

column was a 100 µm inner diameter microcapillary column packed with ~35 cm of Accucore resin (2.6 µm, 150 Å, Sepax). For each analysis, ~2 µg was loaded onto the column. The samples were analyzed by targeted Single Ion Monitoring (t-SIM), with the peptides of interest (heavy and light) defined in an inclusion list by their m/z and charge. The scan sequence began with an Orbitrap MS1 SIM scan for the targeted peptides with an isolation window of 1.7 m/z with the following parameters: resolution of 120,000, AGC target of 1×10^5, maximum injection time of 200 ms, and multiplexing option (MSX) was set to 2 and defined as the pair of heavy and light peptides to be analyzed. This scan was followed by 2 targeted MS2 scans selected from the inclusion list. Each targeted MS2 scan consisted of high-energy collision dissociation (HCD) with the following parameters: resolution of 30,000, AGC of 5×10^4, maximum injection time of 200 ms, isolation window of 1.6 m/z, and normalized collision energy (NCE) of 30. Raw files were imported, and precursor and fragment ions were quantified using Skyline version 3.5. Data generated from Skyline were exported into Excel and PRISM for further analysis. Total PARKIN abundance was determined as the average of the abundance calculated for each individual peptide.

Proteomics - Tandem mass tag labeling

Multiplexing in TMT-based approaches is limited by the number of isobaric tags. To allow comparative studies, we used WT differentiation replicates as bridge channels. Briefly, 50 µg peptides, resuspended in 100 µl of 0.1 M EPPS (pH 8.5) from each sample were labeled with TMT reagent. A total of 5 µL of the 20 ng/µL stock of TMT reagent was added to the peptides along with 25 µL of acetonitrile to achieve a final acetonitrile concentration of approximately 20% (v/v). Following incubation at RT for 1 hour, the reaction was quenched with hydroxylamine to a final concentration of 0.5% (v/v) for 15 min. The TMT-labeled samples were pooled together at a 1:1 ratio. The sample was vacuum centrifuged to near dryness and subjected to C18 solid-phase extraction (SPE) (Sep-Pak, Waters).

Proteomics - Off-line basic pH reversed-phase (BPRP) fractionation

We fractionated the pooled TMT-labeled peptide samples using BPRP HPLC (Wang et al., 2011). We used an Agilent 1100 pump equipped with a degasser and a photodiode array (PDA) detector (set at 220 and 280 nm wavelengths; Thermo Fisher Scientific). Peptides were subjected to a 50-min. linear gradient from 5% to 35% acetonitrile in 10 mM ammonium bicarbonate (pH 8) at a flow rate of 0.8 mL/min. over an Agilent 300Extend C18 column (5 µm particles, 4.6 mm ID and 220 mm in length). The peptide mixture was fractionated into a total of 96 fractions, and concatenated non-consecutively for a total of 12 fractions. Samples were subsequently acidified with 1% formic acid and vacuum centrifuged to near dryness. Each consolidated fraction was desalted via StageTip, dried again via vacuum centrifugation, and reconstituted in 5% acetonitrile, 5% formic acid for LC-MS/MS processing.

Proteomics - Liquid chromatography and tandem mass spectrometry

Mass spectrometry data were collected using an Orbitrap Fusion Lumos mass spectrometer (Thermo Fisher Scientific) coupled to a Proxeon EASY-nLC 1000/1200 liquid chromatography (LC) pump (Thermo Fisher Scientific). The capillary column was a 100 µm inner diameter microcapillary column packed with ~35 cm of Accucore resin (2.6 µm, 150 Å, Sepax). For each analysis, we loaded ~2 µg onto the column.

Each peptide fraction was separated using a 2.5 h gradient of 6 to 26% acetonitrile in 0.125% formic acid at a flow rate of ~450 nL/min. Each analysis used the Multi-Notch MS3-based TMT method (McAlister et al., 2014), a method that reduces ion interference compared to MS2 quantification (Paulo et al., 2016). The scan sequence began with an MS1 spectrum (Orbitrap analysis; resolution 120,000; mass range 400−1400 m/z; automatic gain control (AGC) target 2×10^5; maximum injection time 100 ms). Precursors for MS2 analysis were selected using a

Top10 method. MS2 analysis consisted of collision-induced dissociation (quadrupole ion trap analysis; AGC 4×10^3; normalized collision energy (NCE) 35; maximum injection time 150 ms). Following acquisition of each MS2 spectrum, a synchronous-precursor-selection (SPS) MS3 scan was collected on the top 10 most intense ions in the MS2 spectrum (McAlister et al., 2014). MS3 precursors were fragmented by high energy collision-induced dissociation (HCD) and analyzed using the Orbitrap (NCE 55; AGC 5×10^4; maximum injection time 150 ms, resolution was 60,000 at 200 Th).

Proteomics - Data analysis

Mass spectra were processed using Proteome Discoverer (v2.3.0.420 - Thermo Fisher Scientific). The identification of proteins was performed using the SEQUEST-HT engine against the UniProt Human Reference Proteome (2018 - SwissProt and TrEMBL) using the following parameters (post-recalibration): a tolerance level of 15 ppm for MS^1 and 0.6 Da for MS^2 and false discovery rate of the Percolator decoy database search was set to 1%. Trypsin and LysC were used as the digestion enzyme, two missed cleavages were allowed, and the minimal peptide length was set to 7 amino acids. TMT tags on lysine residues and peptide N termini (+229.163 Da) and carbamidomethylation of cysteine residues (+57.021 Da) were set as static modifications, while oxidation of methionine residues (+15.995 Da) was set as a variable modification. For TMT-based reporter ion quantitation, we extracted (integration tolerance of 0.003 Da) the summed signal-to-noise ratio for each TMT channel and found the closest matching centroid to the expected mass of the TMT reporter ion. For protein-level comparisons, PSMs were identified, quantified, and collapsed to a 1% peptide FDR and then collapsed further to a final protein-level FDR of 1%. Moreover, protein assembly was guided by principles of parsimony to produce the smallest set of proteins necessary to account for all observed peptides. Proteins were quantified by summing reporter ion counts across all matching PSMs unique and razor peptides. PSMs with poor quality, MS^3 spectra with TMT reporter summed signal-to-noise ratio that were less than 10 per channel, isolation specificity ≤0.4, or had less than 70% of correctly selected SPS ions were excluded from quantification (McAlister et al., 2012).

Protein quantification values were exported for further analysis in Microsoft Excel and Perseus (Tyanova et al., 2016). Each reporter ion channel was summed across all quantified proteins and normalized assuming equal protein loading of all 10 samples. Table S1 lists all quantified proteins as well as associated TMT reporter fold change to control channels (WT cells) used for quantitative analysis.

IPA Analysis

The proteomics and transcriptomics datasets included NCBI gene symbols as identifiers, log2 ratios and p-values for each gene. This information was input for IPA using the core analysis platform (Ingenuity Systems). Core analysis settings fold change cut-offs were different for each of our datasets using the following log2 ratios: proteomics pluripotent d0, proteomics DN d35 and transcriptomics DN d35. This was to ensure that the number of enriched or underrepresented proteins/transcripts fell into a similar range and allowed statistically meaningful analysis. IPA generated lists of enriched molecular networks, canonical pathways and biological functions that included disease pathways and that were used to probe dysregulation of pathways previously implicated in PD etiology.

Citations:

Burbulla, L.F., Song, P., Mazzulli, J.R., Zampese, E., Wong, Y.C., Jeon, S., Santos, D.P., Blanz, J., Obermaier, C.D., Strojny, C.*, et al.* (2017). Dopamine oxidation mediates mitochondrial and lysosomal dysfunction in Parkinson's disease. Science *357*, 1255-1261.
Butterfield, D.A., Galvan, V., Lange, M.B., Tang, H., Sowell, R.A., Spilman, P., Fombonne, J., Gorostiza, O., Zhang, J., Sultana, R.*, et al.* (2010). In vivo oxidative stress in brain of Alzheimer disease transgenic mice: Requirement for methionine 35 in amyloid beta-peptide of APP. Free Radic Biol Med *48*, 136-144.
Eden, E., Navon, R., Steinfeld, I., Lipson, D., and Yakhini, Z. (2009). GOrilla: a tool for discovery and visualization of enriched GO terms in ranked gene lists. BMC bioinformatics *10*, 48.
Matsuda, T., and Cepko, C.L. (2007). Controlled expression of transgenes introduced by in vivo electroporation. Proc Natl Acad Sci U S A *104*, 1027-1032.
McAlister, G.C., Huttlin, E.L., Haas, W., Ting, L., Jedrychowski, M.P., Rogers, J.C., Kuhn, K., Pike, I., Grothe, R.A., Blethrow, J.D.*, et al.* (2012). Increasing the multiplexing capacity of TMTs using reporter ion isotopologues with isobaric masses. Analytical chemistry *84*, 7469-7478.
McAlister, G.C., Nusinow, D.P., Jedrychowski, M.P., Wuhr, M., Huttlin, E.L., Erickson, B.K., Rad, R., Haas, W., and Gygi, S.P. (2014). MultiNotch MS3 enables accurate, sensitive, and multiplexed detection of differential expression across cancer cell line proteomes. Analytical chemistry *86*, 7150-7158.
McCarthy, D.J., Chen, Y., and Smyth, G.K. (2012). Differential expression analysis of multifactor RNA-Seq experiments with respect to biological variation. Nucleic Acids Res *40*, 4288-4297.
Paulo, J.A., O'Connell, J.D., and Gygi, S.P. (2016). A Triple Knockout (TKO) Proteomics Standard for Diagnosing Ion Interference in Isobaric Labeling Experiments. Journal of the American Society for Mass Spectrometry *27*, 1620-1625.
Pottier, C., Zhou, X., Perkerson, R.B., 3rd, Baker, M., Jenkins, G.D., Serie, D.J., Ghidoni, R., Benussi, L., Binetti, G., Lopez de Munain, A.*, et al.* (2018). Potential genetic modifiers of disease risk and age at onset in patients with frontotemporal lobar degeneration and GRN mutations: a genome-wide association study. Lancet Neurol *17*, 548-558.
Rigamonti, A., Repetti, G.G., Sun, C., Price, F.D., Reny, D.C., Rapino, F., Weisinger, K., Benkler, C., Peterson, Q.P., Davidow, L.S.*, et al.* (2016). Large-Scale Production of Mature Neurons from Human Pluripotent Stem Cells in a Three-Dimensional Suspension Culture System. Stem cell reports *6*, 993-1008.
Robinson, M.D., McCarthy, D.J., and Smyth, G.K. (2010). edgeR: a Bioconductor package for differential expression analysis of digital gene expression data. Bioinformatics *26*, 139-140.
Surmeier, D.J., Obeso, J.A., and Halliday, G.M. (2017). Selective neuronal vulnerability in Parkinson disease. Nat Rev Neurosci *18*, 101-113.
Tyanova, S., Temu, T., Sinitcyn, P., Carlson, A., Hein, M.Y., Geiger, T., Mann, M., and Cox, J. (2016). The Perseus computational platform for comprehensive analysis of (prote)omics data. Nat Methods *13*, 731-740.
Wang, Y., Yang, F., Gritsenko, M.A., Clauss, T., Liu, T., Shen, Y., Monroe, M.E., Lopez-Ferrer, D., Reno, T., Moore, R.J.*, et al.* (2011). Reversed-phase chromatography with multiple fraction concatenation strategy for proteome profiling of human MCF10A cells. Proteomics *11*, 2019-2026.